PCP
PLANT & CELL PHYSIOLOGY

Dual Targeting of the Protein Methyltransferase PrmA Contributes to Both Chloroplastic and Mitochondrial Ribosomal Protein L11 Methylation in Arabidopsis

Meryl Mazzoleni[1,2,3,4], Sylvie Figuet[1,2,3,4], Jacqueline Martin-Laffon[1,2,3,4], Morgane Mininno[1,2,3,4], Annabelle Gilgen[1,2,3,4], Mélanie Leroux[1,2,3,4], Sabine Brugière[5,6,7], Marianne Tardif[5,6,7], Claude Alban[1,2,3,4] and Stéphane Ravanel[1,2,3,4,*]

[1]Université Grenoble Alpes, Laboratoire de Physiologie Cellulaire & Végétale, F-38041 Grenoble, France
[2]CNRS, UMR5168, F-38054 Grenoble, France
[3]CEA, iRTSV, Laboratoire de Physiologie Cellulaire & Végétale, F-38054 Grenoble, France
[4]INRA, USC1359, F-38054 Grenoble, France
[5]Université Grenoble Alpes, F-38041 Grenoble, France
[6]CEA, iRTSV, Biologie à Grande Echelle, F-38054 Grenoble, France
[7]INSERM, U1038, F-38054 Grenoble, France
*Corresponding author: E-mail, stephane.ravanel@cea.fr; Fax, +33-438785091.
(Received May 15, 2015; Accepted June 22, 2015)

Methylation of ribosomal proteins has long been described in prokaryotes and eukaryotes, but our knowledge about the enzymes responsible for these modifications in plants is scarce. The bacterial protein methyltransferase PrmA catalyzes the trimethylation of ribosomal protein L11 (RPL11) at three distinct sites. The role of these modifications is still unknown. Here, we show that PrmA from *Arabidopsis thaliana* (AtPrmA) is dually targeted to chloroplasts and mitochondria. Mass spectrometry and enzymatic assays indicated that the enzyme methylates RPL11 in plasto- and mitoribosomes in vivo. We determined that the Arabidopsis and *Escherichia coli* PrmA enzymes share similar product specificity, making trimethylated residues, but, despite an evolutionary relationship, display a difference in substrate site specificity. In contrast to the bacterial enzyme that trimethylates the ε-amino group of two lysine residues and the N-terminal α-amino group, AtPrmA methylates only one lysine in the MAFCK(D/E)(F/Y)NA motif of plastidial and mitochondrial RPL11. The plant enzyme possibly methylates the N-terminus of plastidial RPL11, whereas mitochondrial RPL11 is N-α-acetylated by an unknown acetyltransferase. Lastly, we found that an Arabidopsis *prma*-null mutant is viable in standard environmental conditions and no molecular defect could be associated with a lack of RPL11 methylation in leaf chloroplasts or mitochondria. However, the conservation of PrmA during the evolution of photosynthetic eukaryotes together with the location of methylated residues at the binding site of translation factors to ribosomes suggests that RPL11 methylation in plant organelles could be involved, in combination with other post-translational modifications, in optimizing ribosome function.

Keywords: Chloroplast • Dual targeting • Methylation • Mitochondrion • Post-translational modification • Ribosomes.

Abbreviations: AdoMet, *S*-adenosylmethionine; MRPL11, mitochondrial RPL11; MS, mass spectrometry; MS/MS, tandem mass spectrometry; PTM, post-translational modification; PRPL11, plastidial RPL11; RP, ribosomal protein; RT–PC, reverse transcription–PCR.

Introduction

Ribosomes are large ribonucleoprotein complexes that constitute one of the most fundamental molecular machineries in living cells. In eukaryotes, translation of transcripts encoded by the different cellular genomes is catalyzed by ribosomes that are located either in the cytoplasm or in the organelles (mitochondria and plastids). Ribosomes are composed of rRNAs and proteins organized in small and large subunits, although the composition of these subunits varies between eubacterial, cytosolic, mitochondrial and plastidial complexes (Yamaguchi et al. 2000, Yamaguchi and Subramanian 2000, Bonen and Calixte 2006, Carroll 2013). In plastids and mitochondria, translation occurs on prokaryotic-type 70S ribosomes, referred to as plastoribosomes and mitoribosomes, respectively. Their ribosomal proteins (RPs) are encoded by the nuclear and organellar genomes, so that co-ordinated regulation is needed between the three plant genomes for proper assembly of the translation machinery in organelles. Most plastidial RPs and mitochondrial RPs have orthologs in bacteria, reflecting their endosymbiotic heritage. Also, plasto- and mitoribosomes contain a small set of specific proteins with no equivalent in prokaryotic 70S ribosomes (Yamaguchi et al. 2000, Yamaguchi and Subramanian 2000, Bonen and Calixte 2006).

Besides defining the polypeptide composition of ribosomes of diverse origins, protein mass spectrometry (MS) has provided important knowledge about the variety and abundance of post-translational modifications (PTMs) affecting RPs and factors associated with translation. Thus, prokaryotic and eukaryotic

Plant Cell Physiol. 56(9): 1697–1710 (2015) doi:10.1093/pcp/pcv098, Advance Access publication on 26 June 2015, available FREE online at www.pcp.oxfordjournals.org

RPs are subjected to a plethora of PTMs including initiator methionine removal, phosphorylation, acetylation or methylation (e.g. Yamaguchi et al. 2000, Yamaguchi and Subramanian 2000, Polevoda and Sherman 2007, Carroll et al. 2008, Nesterchuk et al. 2011, Koc and Koc 2012). Some of these PTMs have been conserved during evolution, suggesting that they could be important for ribosomal assembly and/or function. However, little progress has been made in identifying the enzymes involved and in understanding the functional significance of these covalent modifications (Nesterchuk et al. 2011, Koc and Koc 2012, Carroll 2013).

Methylation of the cytoplasmic translation apparatus in yeast has been studied extensively. Several protein methyltransferases from *Saccharomyces cerevisiae* acting on either lysine, arginine, histidine or the N-terminal residue of several RPs have been characterized (e.g. Chern et al. 2002, Porras-Yakushi et al. 2005, Webb et al. 2010a, Webb et al. 2010b, Young et al. 2012). They modify proteins from the small (Rps3, Rps2, Rps25 and Rps27) and large (Rpl1, Rpl3, Rpl12, Rpl23 and Rpl42) subunits, and methylated sites are exposed at the surface or buried deeply within the ribosomal structure (Clarke 2013). In most cases, the functional consequences of methylation are not known. Only recently, methylation of Rpl3 by the Hpm1 methyltransferase has been shown to be required for proper assembly of the large ribosomal subunit and translation initiation in *S. cerevisiae* (Al-Hadid et al. 2014). Methylation of the bacterial or organellar RPs is less documented. The methyltransferases PrmA and PrmB that are specific to RPL11 and RPL3, respectively, have been identified in bacteria. PrmB is a protein glutamine methyltransferase specific to RPL3; it is important for ribosomal assembly but not for its stability or activity (Nesterchuk et al. 2011). PrmA has a unique property in that it is able to catalyze the N-ε-trimethylation of two internal lysine residues as well as the N-α-trimethylation of the N-terminal alanine residue of RPL11 (Dognin and Wittmann-Liebold 1980). PrmA consists of a C-terminal catalytic domain with a canonical seven-β-strand structural fold and an N-terminal domain involved in substrate recognition. Extensive structural analysis of PrmA–RPL11 complexes indicated that (i) the binding mode remains conserved in all RPL11 orientations; and (ii) the linker region comprised between the two domains is highly flexible and enables several substrate orientations with respect to the methyltransferase catalytic site (Demirci et al. 2007, Demirci et al. 2008). The methylated residues of RPL11 are located in the N-terminal domain of the protein, which is known to interact with initiation, elongation and release factors. It has been suggested, therefore, that these modifications could be important to control binding of protein synthesis factors (Polevoda and Sherman 2007). Also, because dissociated RPs serve as much better substrates for in vitro methylation by PrmA than intact 70S ribosomes, it has been proposed that methylation could occur before the assembly of the large subunit and thus play a role in ribosome biogenesis (Cameron et al. 2004). To date, the role of RPL11 methylation is not known as *prmA*-null mutants from *E. coli* or *Thermus thermophilus* are viable and show no obvious phenotype (Vanet et al. 1994, Cameron et al. 2004).

Methylation marks have been detected in several cytoplasmic or plastidial RPs from plants (Yamaguchi et al. 2000, Yamaguchi and Subramanian 2000, Carroll et al. 2008). These N-terminal or internal modifications are specific to plant proteins or have been conserved during evolution (e.g. methylation of RPL11 from spinach plastoribosomes). During the inventory of lysine- and arginine-methylated proteins in Arabidopsis chloroplasts, we also identified a trimethylated internal lysine residue in plastidial RPL11 (PRPL11; Alban et al. 2014). Moreover, we determined that the Arabidopsis protein methyltransferase AtPrmA, orthologous to bacterial PrmA, was able to catalyze the trimethylation of a recombinant PRPL11 from Arabidopsis at this particular lysine residue. In the present study, we show that AtPrmA is dual targeted to both plastids and mitochondria. Methylation assays and MS analyses performed with the wild type [Columbia (Col-0)] and a *prma*-null mutant indicated that the enzyme is capable of methylating PRPL11 and mitochondrial RPL11 (MRPL11) in vivo. We also show that, despite their evolutionary relationship, bacterial and plant PrmA display different substrate site specificity. Lastly, we found that the Arabidopsis *prma*-null mutant is viable under standard growth conditions and displays no obvious phenotype. However, the conservation of PrmA during the evolution of photosynthetic eukaryotes (plants, and green, red and chromist algae) together with the location of methylated residues at the surface of ribosomes suggests that RPL11 methylation in organelles could have a role in binding of translation factors.

Results

Isolation and genetic complementation of an Arabidopsis *prma* null mutant

To explore the function of AtPrmA in vivo, an Arabidopsis mutant carrying a T-DNA insertion in the At5g53920 locus was identified and confirmed by sequencing. The insertion interrupted the open reading frame in the sixth exon, 245 residues downstream from the start codon (**Fig. 1A**). Reverse transcription–PCR (RT–PCR) analyses and immunoblotting showed that this line, designated *prma*, is a loss-of-function allele that lacks the PRMA transcript and protein (**Fig. 1B, C**). Growth of *prma* during both vegetative and reproductive development did not differ visually from that of the wild type under standard long- or short-day conditions. Thus, as previously observed in bacteria (Vanet et al. 1994, Cameron et al. 2004), the function of PrmA is dispensable in Arabidopsis under these conditions.

To analyze whether the *prma*-null mutation was associated with a defect in protein methylation, we performed in vitro methylation assays using recombinant AtPrmA and total soluble leaf protein extracts from either *prma* or Col-0 as substrates. As shown in **Fig. 1D**, the incorporation of ^{3}H-labeled methyl groups into proteins was about 20 times higher in *prma* than in the wild type. The main labeled polypeptide(s) was detected at 17 ± 2 kDa by SDS–PAGE and autoradiography, a molecular mass that is expected for RPL11 proteins

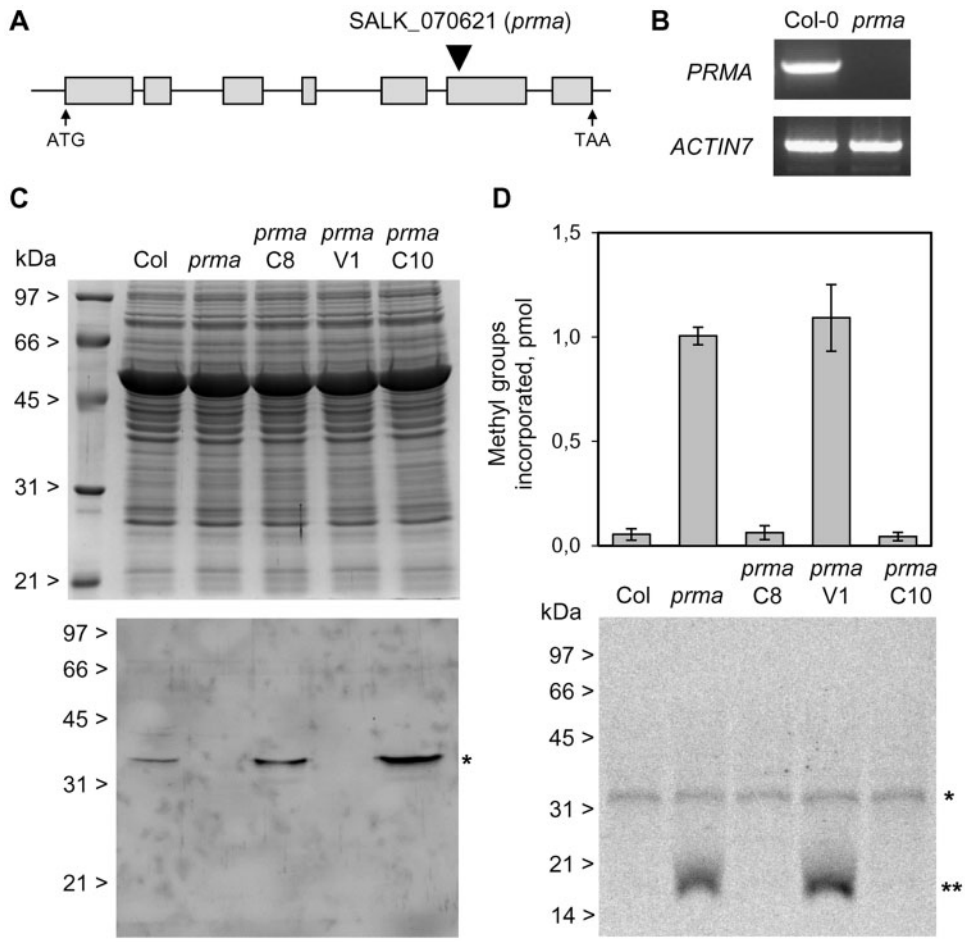

Fig. 1 Isolation and genetic complementation of an Arabidopsis *prma* null mutant. (A) Schematic view of the *PRMA* (At5g53920) locus with exons as gray boxes and the T-DNA insertion indicated by a black triangle. (B) Expression of the *PRMA* transcript in the *prma* and wild-type (Col-0) lines. The *ACTIN7* gene (At5g09810) served as an internal control for RT–PCR experiments. (C) Expression of the AtPrmA protein in Col-0, *prma* and *prma* complemented lines. The *prma*-null mutant was transformed with a *35S::PRMA* construct in plasmid pFP101, leading to the T_2 homozygous lines *prma 35S::PRMA* C8 and C10. The *prma* V1 line was obtained by transformation with an empty vector. Soluble proteins (30 μg) were prepared from leaves and analyzed by Western blot using antibodies against recombinant AtPrmA. (D) In vitro methylation of soluble proteins from Col-0, *prma* and *prma* complemented lines by AtPrmA. Soluble proteins (25 μg) from leaves were used as substrates for methylation assays with 20 μM [methyl-^{3}H]AdoMet and recombinant AtPrmA (4 μg). After incubation at 30°C for 3 h, proteins were either precipitated to count incorporated methyl groups (upper panel) or resolved by SDS–PAGE and used for phosphorimage analysis (lower panel). Values are the mean ± SEM of three replicates. The positions of AtPrmA (*34 kDa, automethylation) and RPL11 (**17 kDa) are indicated.

(the calculated M_rs of mature Arabidopsis PRPL11 and MRPL11 are about 17,000 kDa). These data suggested that the substrate(s) of AtPrmA is nearly fully methylated in vivo in leaves of wild-type plants whereas it is not (or poorly) methylated in *prma*. To analyze whether the substrates of AtPrmA are PRPL11 and/or MRPL11, in vitro methylation assays have been done using total soluble leaf proteins from the *prpl11* and *mrpl11* knockout lines (Pesaresi et al. 2001, Pesaresi et al. 2006). No incorporation of methyl groups could be observed at 17 kDa using the *prpl11* protein extract, whereas labeling at this molecular mass was comparable in *mrpl11* and Col-0 (**Supplementary Fig. S1**). These results indicate that PRPL11 at least is a substrate of recombinant AtPrmA in total soluble leaf extracts.

To confirm further that the lack of the AtPrmA protein was responsible for the methylation-deficient phenotype of the null mutant, we introduced the full-length At5g53920 open reading frame driven by a double 35S *Cauliflower mosaic virus* (CaMV) promoter into the *prma* background. Homozygous T_2 complemented lines designated *prma 35S::PRMA* C8 and C10 were selected and shown to express AtPrmA at substantially higher level than the wild type in leaf extracts (**Fig. 1C**). Complemented plants were normal in appearance when grown under regular environmental conditions. Incorporation of methyl groups in soluble proteins extracted from *prma 35S::PRMA* C8 and C10 lines using recombinant AtPrmA was low and comparable with that measured from Col-0 extracts, indicating that complementation rescued the ability of *prma* to methylate the RPL11 polypeptide(s) at 17 kDa in vivo (**Fig. 1D**). These data, together with the previous demonstration that recombinant AtPrmA enzyme is able to methylate recombinant PRPL11 from Arabidopsis in vitro (Alban et al. 2014), indicate that AtPrmA is required for methylation of RPL11 proteins from plastids and/or mitochondria in vivo.

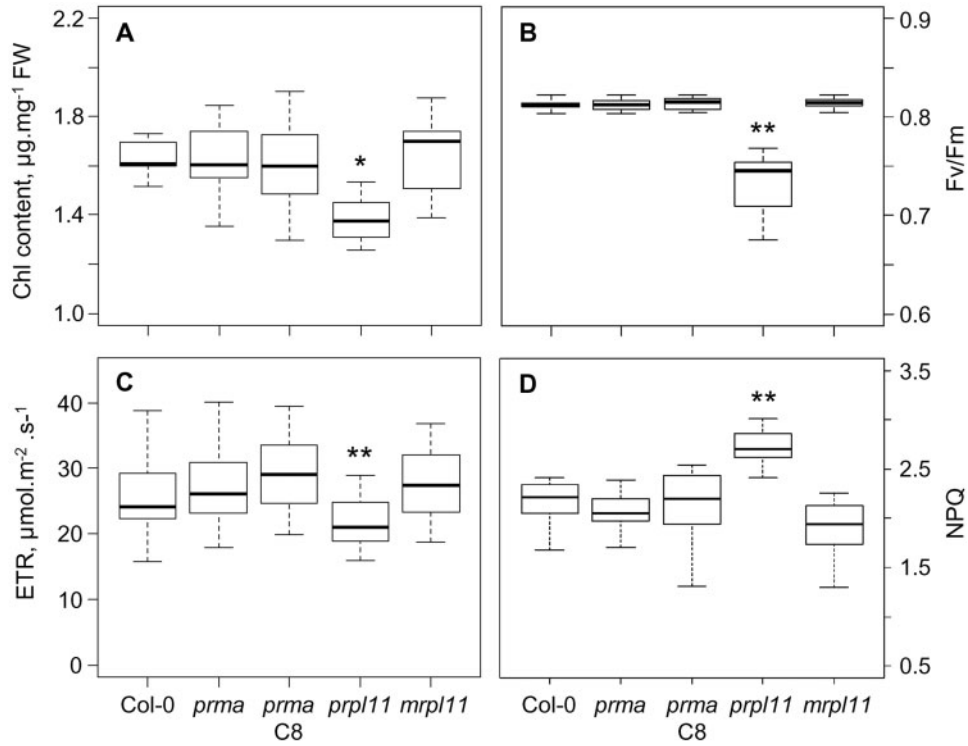

Fig. 2 Photosynthetic parameters of the *prma* mutant. Chl content (A) and photosynthetic parameters (B–D) were determined in leaves from 3-week-old Col-0, *prma*, *prma 35S::PRMA* C8, *prpl11* and *mrpl11* seedlings. Recorded photosynthetic parameters were the efficiency of PSII in dark-adapted leaves (F_v/F_m), the electron transfer rate (ETR; calculated from the quantum efficiency of PSII in the light) and non-photochemical quenching (NPQ). The data represent three independent cultures analyzed in five replicates for pigment analysis and >20 replicates for photosynthetic parameters. Statistical analysis was performed using Kruskal–Wallis test followed by Mann–Whitney test, with $P < 0.05$ (*) and $P < 0.01$ (**) compared with Col-0.

Characterization of the *prma* mutant

Deletion of genes coding for protein methyltransferases involved in the modification of RPs and translation factors usually do not cause major phenotypes and, in most cases, the functional role of methylation is not known (Polevoda and Sherman 2007, Clarke 2013). Thus, a defect in RPL11 methylation in bacteria is not accompanied by any dysfunction of the ribosomal machinery (Vanet et al. 1994, Cameron et al. 2004), but a deletion of the *rplK* gene encoding RPL11, although not lethal, causes a significant reduction in the rate of in vitro protein synthesis and an increased generation time (Stark and Cundliffe 1979). Similarly, the lack of PRPL11 and MRPL11 in Arabidopsis is not essential but has been associated with diverse phenotypic effects originating from a reduction in the efficiency of protein synthesis in the organelles (Pesaresi et al. 2001, Pesaresi et al. 2006). Thus, the rate of translation of plastid-encoded proteins is significantly reduced in the *prpl11* mutant, leading to pale green seedlings with a decreased growth rate and increased photosensitivity (Pesaresi et al. 2001). In the *mrpl11* mutant, impairment of mitochondrial protein synthesis was associated with a reduction in size and a darker coloration of leaves (Pesaresi et al. 2006).

To determine whether the *prma* mutation could result in molecular and physiological defects similar to those observed for *prpl11* or *mrpl11*, we analyzed these three mutants together with Col-0 and the *prma 35S::PRMA* C8 complemented line. First, we determined pigment content and analyzed photosynthetic performance of leaves from 3-week-old seedlings. As mentioned previously, the *prma*-null mutant could not be distinguished from Col-0 under these conditions although the phenotypic defects of *prpl11* and *mrpl11* were observed. As shown in **Fig. 2A**, only *prpl11* displayed a significant change in Chl content, with a decrease of about 15% as compared with Col-0. Monitoring of Chl fluorescence in vivo allowed us to analyze the efficiency of PSII in dark-adapted leaves (F_v/F_m), the quantum efficiency of PSII and the electron transfer rate in the light, and non-photochemical quenching (**Fig. 2B–D**). These parameters were comparable in Col-0, *prma*, *prma 35S::PRMA* lines and *mrpl11*. Only the *prpl11* mutant displayed a marked impairment in photosynthetic electron flow and increased photoinhibition, as previously reported (Pesaresi et al. 2001). Immunoblot analyses were then conducted to determine whether the protein composition of chloroplasts and mitochondria was altered in *prma*. With this aim, we have probed protein extracts from leaves using antibodies against soluble and membrane proteins encoded by either the nuclear, plastid or mitochondrial genome. The results shown in **Fig. 3** indicated a significant reduction in the level of plastid-encoded proteins in *prpl11* and a slight decrease of mitochondrion-encoded proteins in *mrpl11*, as reported in previous studies (Pesaresi et al. 2001, Pesaresi et al. 2006). The steady-state level of these proteins and those encoded by

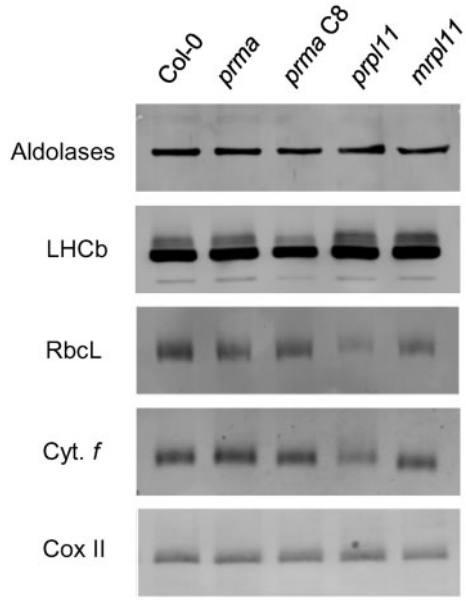

Fig. 3 Steady-state level of chloroplastic and mitochondrial proteins in the *prma* mutant. Soluble and membrane proteins were extracted from leaves of 3-week-old seedlings, resolved by SDS–PAGE and transferred to nitrocellulose. Membranes were probed with antibodies against nuclear-encoded chloroplastic proteins [fructose 1,6 bisphosphate aldolases, light-harvesting antenna complex II (LHCb)], plastid-encoded proteins [Rubisco large subunit (RbcL), Cyt *f*] or a mitochondrial-encoded protein [cytochrome oxidase subunit II (Cox II)].

the nuclear genome did not differ significantly between Col-0 and *prma*. Together, these data indicate that a lack of *PRMA* in Arabidopsis leaves does not mimic the phenotypic and molecular abnormalities observed in *prpl11* or *mrpl11* mutants.

We also analyzed the effect of the *prma* mutation on seed germination. This complex process corresponds to the transition from a quiescent to a proliferative metabolic state and requires a high rate of protein synthesis and ribosome turnover (Rajjou et al. 2012). Translation of stored mRNA by cytoplasmic 80S ribosomes is critical during Arabidopsis seed germination (Rajjou et al. 2004, Galland et al. 2014), but little is known about the importance of organellar translation during this process. To investigate this role, we tested the effect of two inhibitors of prokaryotic 70S ribosomes on the germination of Arabidopsis seeds. Under our experimental conditions, germination (radicle protrusion) of Col-0 seeds on distilled water started after 25 ± 3 h of imbibition, and 50% of the seed population reached this stage after 34 ± 4 h (**Fig. 4A**). In the presence of cycloheximide, an inhibitor of cytoplasmic ribosomes, germination was fully abolished, as previously described (Rajjou et al. 2004). For chloramphenicol and spectinomycin, which interfere with peptide bond formation and the translocation reaction on prokaryotic ribosomes, respectively, germination was significantly delayed but not stopped (**Fig. 4A**). After completion of germination, seedlings were albinos and growth was arrested, indicating that plastid differentiation into chloroplast was blocked and that inhibition of protein synthesis by the antibiotics was efficient, at least in plastids. Together, these data suggested that germination sensu stricto does not have an absolute requirement for protein synthesis in organelles. Germination assays of the *prma*, *prpl11* and *mrpl11* mutants were performed on distilled water. No significant delay in germination could be observed between these lines and Col-0 or *prma 35S::PRMA* transformants (**Fig. 4B**), indicating, therefore, that PrmA, PRPL11 and MRPL11 are not essential to this process in Arabidopsis.

Dual targeting of AtPrmA in both chloroplasts and mitochondria

AtPrmA together with 19 orthologous proteins identified in the genomes from higher plants (Phytozome database, v9.1) showed N-terminal extensions as compared with bacterial PrmA proteins. The subcellular localization of plant PrmA proteins was analyzed using dedicated prediction softwares (Emanuelsson et al. 2000, Small et al. 2004, Kaundal et al. 2010, Tanz et al. 2013). These tools identified transit peptide-like sequences in these proteins and suggested a possible targeting to plastids and/or mitochondria. This prediction was strengthened by using the ambiguous targeting predictor (Mitschke et al. 2009), which indicated significant probability (scores ranging from 0.51 to 0.91) for plant PrmA proteins to be dually targeted to plastids and mitochondria. To verify these predictions, we analyzed the subcellular distribution of AtPrmA by Western blot using antibodies raised against the recombinant protein. Chloroplasts and mitochondria were purified from Arabidopsis leaves using Percoll density gradients, providing organelles at high levels of purity (<1% cross-contamination of chloroplasts by mitochondrial markers, 3–5% cross-contamination of mitochondria by plastidial markers) (**Fig. 5**; **Supplementary Fig. S2**). AtPrmA was detected as a 34 kDa polypeptide in both the chloroplast stroma and mitochondrial matrix (**Fig. 5**). This molecular mass was expected for a mature AtPrmA protein devoid of its transit peptide leader sequence (Alban et al. 2014). A cytosolic-enriched fraction was also probed with the antibodies, and the very faint signal obtained was attributed to the cross-contamination of cytosol by plastidial (~7%) and mitochondrial (<1%) proteins (Puyaubert et al. 2008). To strengthen these data, we measured the ability of stromal and matrix fractions isolated from Col-0 plants to methylate recombinant Arabidopsis PRPL11 (Alban et al. 2014). As shown in **Fig. 6A**, both fractions were able to methylate AtPRPL11, whereas stroma and matrix isolated from *prma* plants have lost this capacity. Together, these data indicate that AtPrmA is dual localized and active in both chloroplasts and mitochondria.

Methylation of PRPL11 and MRPL11 by AtPrmA in vivo

We have shown previously that native RPL11 from Arabidopsis chloroplasts is trimethylated at Lys109 and that AtPrmA is able to methylate recombinant AtPRPL11 at this site in vitro (Alban et al. 2014). The presence of an active PrmA enzyme in the mitochondrial matrix suggested strongly that RPL11 from mitoribosomes could also be methylated at one or several positions. All our attempts to produce recombinant Arabidopsis MRPL11 in *E. coli* cells failed, and thus we could not analyze the

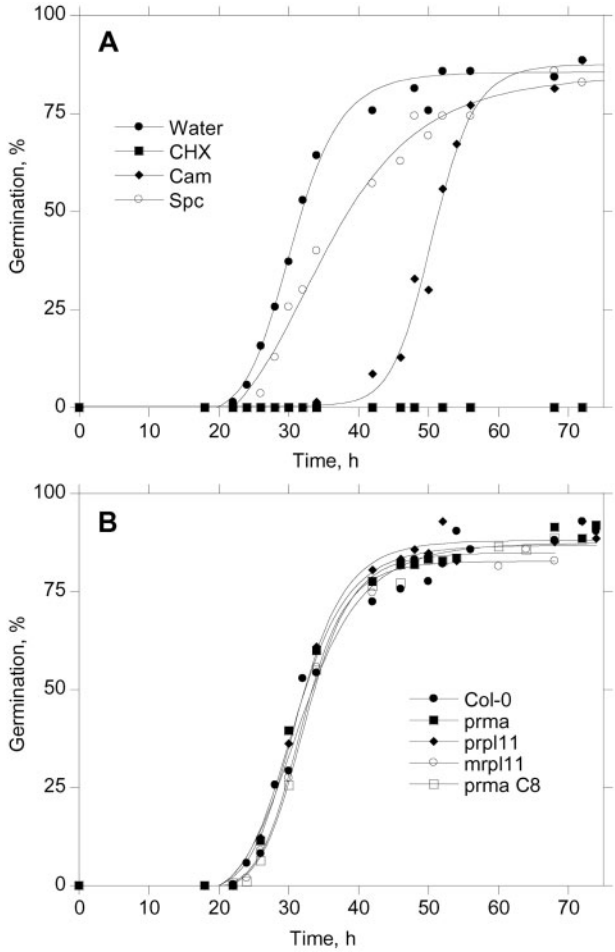

Fig. 4 Effect of translation inhibitors and mutations affecting the ribosomal machinery on seed germination. (A) Effect of translation inhibitors on the germination of Col-0 seeds. Seeds were incubated on absorbent paper imbibed with either distilled water, cycloheximide (CHX, 0.1 mM), chloramphenicol (Cam, 0.6 mM) or spectinomycin (Spc, 1 mM). (B) Germination of seeds from Col-0, *prma* and other mutant lines on water. Germination was carried out at 23°C under continuous light. A seed was regarded as germinated when the radicle protruded through the seed coat. Each germination assay was performed in duplicate (70 seeds per analysis). Curves displayed in (B) are representative of germination kinetics done with four independent seed lots harvested over a 2 year period. Curves were fitted by using the equation described in Joosen et al. (2010) and the Kaleidagraph software.

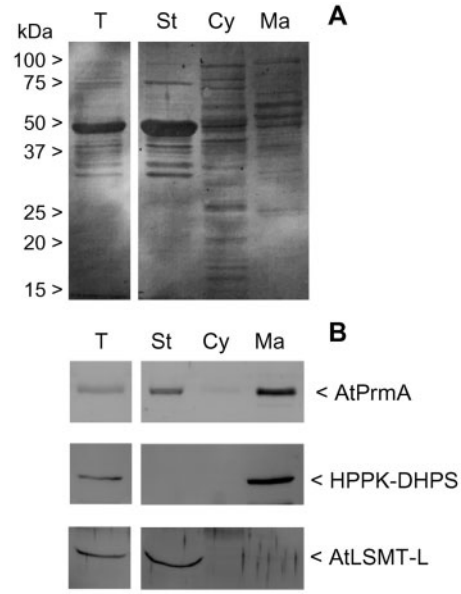

Fig. 5 Subcellular localization of AtPrmA. Immunoblot analyses were performed using proteins (Col-0 ecotype) from a total soluble leaf extract (T), stroma from purified chloroplasts (St), matrix from purified mitochondria (Ma) and a cytosolic-enriched fraction (Cy). Proteins (20 μg per lane) were resolved by SDS–PAGE, transferred to nitrocellulose, stained with Ponceau S (A), and analyzed with polyclonal antibodies against AtPrmA (B). Membranes were also probed with antisera against HPPK-DHPS (mitochondrial marker, 52 kDa) (Mouillon et al. 2002) and AtLSMT-L (chloroplastic marker, 50 kDa) (Mininno et al. 2012). Additional information about organelle purity is provided in **Supplementary Fig. S2**.

ability of AtPrmA to modify this target in vitro. To bypass this problem, we measured the AtPrmA-dependent incorporation of methyl groups into chloroplastic and mitochondrial proteins from either the wild type or the *prma*-null mutant. Methylation assays with stromal proteins revealed a single labeled polypeptide of about 17 kDa (**Fig. 6B**). The incorporation of methyl-^{3}H from *S*-adenosylmethionine (AdoMet) was much higher in *prma* than in Col-0, indicating that in Arabidopsis leaves most of the PRPL11 pool is methylated by PrmA. Using the same approach, two polypeptides with very similar M_rs were detected in the matrix from *prma* mitochondria, whereas no signal could be detected in proteins from wild-type mitochondria (**Fig. 6B**). The upper polypeptide of the doublet migrated at the same position as PRPL11 and could be due to the cross-contamination of Percoll-purified mitochondria by chloroplast proteins (3–5%; **Supplementary Fig. S2**). The lower polypeptide was not observed in stromal fractions and probably corresponds to MRPL11.

To confirm the identity of proteins methylated by PrmA in vivo and to identify methylation sites, we performed tandem mass spectrometry (MS/MS) analyses. To this aim, stroma and matrix proteins from either Col-0 or *prma* were resolved by SDS–PAGE and protein bands containing RPL11 (range 15–20 kDa) were excised from the gel. Proteins were digested by trypsin and submitted to nano-LC-MS/MS using an LTQ-Orbitrap mass spectrometer. To identify methylpeptides, MS/MS spectra were searched for mass shifts corresponding to mono-, di- and trimethylation of lysine residues using the procedure described previously (Mininno et al. 2012, Alban et al. 2014). In Col-0 and *prma*, PRPL11 was one of the most abundant proteins identified in gel pieces excised from stroma samples, and 10 peptides were identified with a sequence coverage of 45%. In Col-0, a unique methylation site was identified at Lys109. The most intense peptide ions covering this residue (94% of the intensity) were found to be trimethylated at Lys109 whereas a second less intense peptide was not modified at this position (**Table 1**; **Supplementary Fig. S3**). In *prma*, these two peptides were also detected and found to be unmethylated at Lys109. These data are in accordance with the activities described in **Fig. 6B**, and demonstrate that PrmA is involved in the methylation of PRPL11 at Lys109 in vivo.

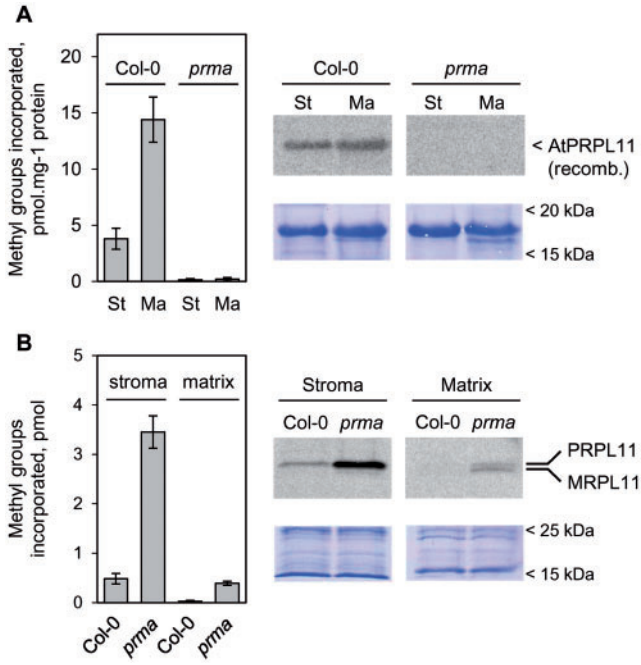

Fig. 6 AtPrmA methylates RPL11 in both chloroplasts and mitochondria. (A) Activity of native AtPrmA from chloroplasts and mitochondria using AtPRPL11 as a substrate. Recombinant AtPRPL11 (5 μg) was used as a substrate for methylation assays with 20 μM [methyl-^{3}H]AdoMet and stroma (St) or matrix (Ma) proteins (25 μg) as sources of methyltransferases. After incubation at 30°C for 4 h, methyl groups incorporated into proteins were counted and analyzed by phosphorimaging. Values are the mean ± SEM of three replicates. The molecular mass of recombinant 6 × His-tagged AtPRPL11 is 17.9 kDa. (B) Activity of recombinant AtPrmA using stroma and matrix extracts as substrates. Stroma and matrix proteins (25 μg) were used as substrates for methylation assays with 20 μM [methyl-^{3}H]AdoMet and recombinant AtPrmA (4 μg). Incubation time and sample treatments were as above. The molecular mass of methylated RPL11 substrates is about 17 kDa.

Unlike PRPL11, we found that MRPL11 is not an abundant protein in the mitochondrial matrix. This is in agreement with the low level of incorporation of methyl groups observed in the extract from *prma* mitochondrial matrix as compared with *prma* chloroplast stroma (**Fig. 6B**). Also, peptides belonging to PRPL11 were identified in mitochondrial samples, supporting the in vitro labeling pattern observed in **Fig. 6B**. A first analysis of MS/MS spectra from the Col-0 sample did not identify any methylated peptide, probably because of the low abundance and weak sequence coverage of MRPL11. To overcome this limitation, a new analysis was performed using an Inclusion List of peptides that contain Lys48 (**Supplementary Fig. S3**), which is predicted to be a methylation site of MRPL11 (**Supplementary Fig. S4**). Using these parameters, 10 peptides from MRPL11 were retrieved in the Col-0 sample, of which one contained a trimethylated lysine at position 48 (**Table 1**; **Supplementary Fig. S3**). It is noteworthy that a peptide covering the N-terminus of MRPL11 was found to be N-α-acetylated at Ala2. This finding identifies the true N-terminus of the protein and indicates that MRPL11 is targeted to mitochondria without a cleavable transit peptide (see **Supplementary Fig. S4**). In mitochondria from *prma* leaves, MRPL11 was identified from seven peptides (coverage of 44%), none of which was bearing a PTM. In particular, the Lys48 residue was found to be unmodified (**Table 1**; **Supplementary Fig. S3**). These data indicate that AtPrmA is able to trimethylate the Lys48 residue of MRPL11 in vivo at a site that is highly conserved in RPL11 proteins from bacteria, plastids and mitochondria (**Supplementary Fig. S4**).

Biochemical characterization of AtPrmA

In *E. coli*, PrmA exhibits an unusual substrate site specificity since it is able to introduce nine methyl groups at three distinct positions of the RPL11 protein (Dognin and Wittmann-Liebold 1980). To examine whether AtPrmA conserved this unique property, we performed kinetic analysis of the recombinant enzyme using AtPRPL11 as a substrate. We have reported previously that methylation of AtPRPL11 was dependent on time and enzyme concentration (Alban et al. 2014). Here, we showed that prolonged incubation periods (>2 h in our conditions) resulted in the incorporation of three methyl groups per protein substrate (525 ± 30 pmol of methyl for 170 pmol of AtPRPL11; **Fig. 7A**). To decipher whether the difference in stoichiometry catalyzed by bacterial and plant methyltransferases was attributable to divergent properties of the enzymes or to the nature of the substrate, we purified a recombinant *E. coli* PrmA (EcPrmA) and generated two point mutants of Arabidopsis PRPL11. Mutations on AtPRPL11 introduced non-methylatable alanine residues in place of Lys73 or Lys109, which correspond to the trimethylated lysine residues in RPL11 from *E. coli* (**Supplementary Fig. S4**). Methylation of wild-type AtPRPL11 by EcPrmA resulted in biphasic kinetics, with a fast initial incorporation of three methyl groups per protein substrate followed by a slower incorporation of three additional methyl groups (**Fig. 7B**). Mutation of Lys109 to alanine on AtPRPL11 fully abolished the methylation process by AtPrmA and resulted in a slow incorporation of three methyl groups with EcPrmA (**Fig. 7A, B**). Time-courses with the AtPRPL11 K73A mutant displayed a similar behavior to that of the wild-type substrate for AtPrmA and suppressed the second phase of methyl incorporation by EcPrmA. Together, the results obtained with the Arabidopsis enzyme suggest a unique site of trimethylation located on Lys109, which is consistent with the identification of this residue as a methylation site of PRPL11 in vivo (**Table 1**). These data also indicate that EcPrmA is able to methylate Lys109 rapidly on recombinant AtPRPL11 and, once this site is almost stoichiometrically occupied by methyl groups, to trimethylate Lys73 with a lower efficiency.

To understand why EcPrmA was only able to introduce six methyl groups on AtPRPL11 instead of the expected nine (Dognin and Wittmann-Liebold 1980), we determined the N-terminal sequence of the protein by Edman microsequencing. The obtained sequence (Pro-Pro-Lys-Pro-Gly) indicated that the first two residues (Met-Ala) of recombinant AtPRPL11 had been processed during maturation of the protein in *E. coli* cells. Thus, the presence of an N-terminal proline

Table 1 Properties of peptides covering the methylation sites of PRPL11 and MRPL11 in the wild-type and *prma* genetic backgrounds

Genotype	Peptide	Sequence	Modification	Mass measured	Mass calculated	Charge	Delta (p.p.m.)	Mascot score (best)	Precursor intensity (%)
PRPL11 (At1g32990)									
Col-0	101–109	GVNIMAFCK	–	528.2542	1,054.4940	2	−0.14	45.42	6.38
	101–114	GVNIMAFCKDYNAR	$K109_{me3}$	567.6113	1,699.8174	3	−0.30	53.19	93.62
prma	101–109	GVNIMAFCK	–	528.2533	1,054.4940	2	−1.83	50.82	94.89
	101–114	GVNIMAFCKDYNAR	–	837.8903	1,673.7654	2	0.35	62.03	5.11
MRPL11 (At4g35490)									
Col-0	41–53	LNLMAFCKDFNAR	$K48_{me3}$	547.9465	1,640.8167	3	0.62	41.64	100
prma	41–48	LNLMAFCK	–	498.7538	995.4932	2	−0.20	52.13	100

Stroma and matrix fractions obtained from purified organelles were resolved by SDS–PAGE and tryptic peptides were generated from the excised 15–20 kDa protein bands. MS/MS spectra were obtained using an LTQ-Orbitrap mass spectrometer and data were searched for methylpeptides (see the Materials and Methods). Precursor intensity is an estimation based on the sum of the intensity of the selected parent ions bearing the lysyl residue of interest. Representative MS/MS spectra are available in **Supplementary Fig. S3**.

residue on the recombinant substrate precluded analyzing the ability of EcPrmA and AtPrmA to modify the α-amino group of the N-terminal amino acid of AtPRPL11. To bypass this limitation, we purified a recombinantly expressed RPL11 from *E. coli* (EcRPL11) and verified by sequencing that the α-NH_2 of the protein was free and methylatable. This was the case since the N-terminal sequence was Ala-Lys-Lys-Val-Gln. Methylation assays with either AtPrmA or EcPrmA displayed monophasic curves of methyl group incorporation into EcRPL11 (**Fig. 7C**). A stoichiometry of six and nine methyl groups per protein substrate was calculated with AtPrmA and EcPrmA enzymes, respectively (260 ± 20 vs. 400 ± 40 pmol of methyl for 45 pmol of EcRPL11). These data indicate that recombinant EcPrmA trimethylates three distinct sites of EcRPL11, like the native enzyme (Dognin and Wittmann-Liebold 1980). Together with results from **Fig. 7A**, these data also suggest that AtPrmA catalyzes the trimethylation of the distal Lys40 and the α-amino group of the N-terminal alanine residue of EcRPL11.

Phylogenetic analysis of PrmA proteins

In order to explore the evolutionary origin of PrmA in plants, we performed BlastP searches to identify orthologs in a wide range of organisms. PrmA orthologs were identified in all bacterial phyla, as expected from the previous characterization of the enzyme in *E. coli* (proteobacteria phylum) and *T. thermophilus* (Deinococcus-Thermus phylum) (Vanet et al. 1994, Cameron et al. 2004), but not in archaea. In eukaryotes, orthologous sequences were found exclusively in Viridiplantae (land plants and green algae), glaucophytes, rhodophytes (red algae) and chromists (algae that include diatoms or haptophytes). In other eukaryotes (mammals, fungi or apicomplexa, which are closely related to chromists but did not retain a photosynthetic plastid), best hits from the BlastP searches matched only with the C-terminal catalytic domain of PrmA but lacked significant homology with the N-terminus that is involved in binding of the RPL11 substrate. These proteins are probably methyltransferases with a seven-β-strand structural fold, although they are not RPL11 methyltransferases. It seems, therefore, that the PrmA protein is restricted to bacteria and photosynthetic eukaryotes (the presence of a PrmA in euglenids could not be ascertained since genomic data are very limited for these photosynthetic organisms). This suggested that the *PRMA* gene could have been inherited by endosymbiotic gene transfer from the cyanobacterium to the nuclear genome of photosynthetic eukaryotes. Indeed, cyanobacteria are at the origin of plastids in Plantae (land plants, green algae, glaucophytes and red algae) via primary endosymbiosis, while plastids in other eukaryotes (chromists, euglenids) are believed to have derived from red algae during subsequent endosymbiotic events (Dorrell and Smith 2011, Stiller et al. 2014). Phylogenetic analysis showed that PrmA orthologs are clustered into three distinct clades: bacteria, Viridiplantae/glaucophytes and red/chromist algae (**Fig. 8**). Among bacterial phyla, PrmA proteins with the highest homology to eukaryotic proteins were found in β- and γ-proteobacteria. Since branching between prokaryotic phyla and eukaryotic clades was not supported by consistent bootstrap values (**Fig. 8**), it is not possible to conclude from these analyses whether PrmA found in photosynthetic eukaryotes is derived from cyanobacteria by endosymbiotic gene transfer or from other bacteria, probably proteobacteria, by lateral gene transfer.

Discussion

In the present study, we show that the protein methyltransferase PrmA encoded by a unique gene (At5g53920) in Arabidopsis is dually targeted to both chloroplasts and mitochondria. We also demonstrate that the enzyme is active in these cellular compartments where it catalyzes the methylation of either PRPL11 or MRPL11. Over 100 plant proteins have been found to be dual targeted to chloroplasts and mitochondria (Carrie and Small 2013). These proteins fall in a limited number of essential cellular processes, including tRNA synthesis and translation (e.g. aminoacyl-tRNA synthetases, RPs or processing enzymes). The presence of PrmA in the pool of dual-targeted proteins suggests that the enzyme has been selected during evolution to provide a function in both organelles, as suggested for other components of the translational machinery (Carrie and Small 2013). It has been shown previously that a complex transcriptional and splicing control of the Arabidopsis *PIMT2*

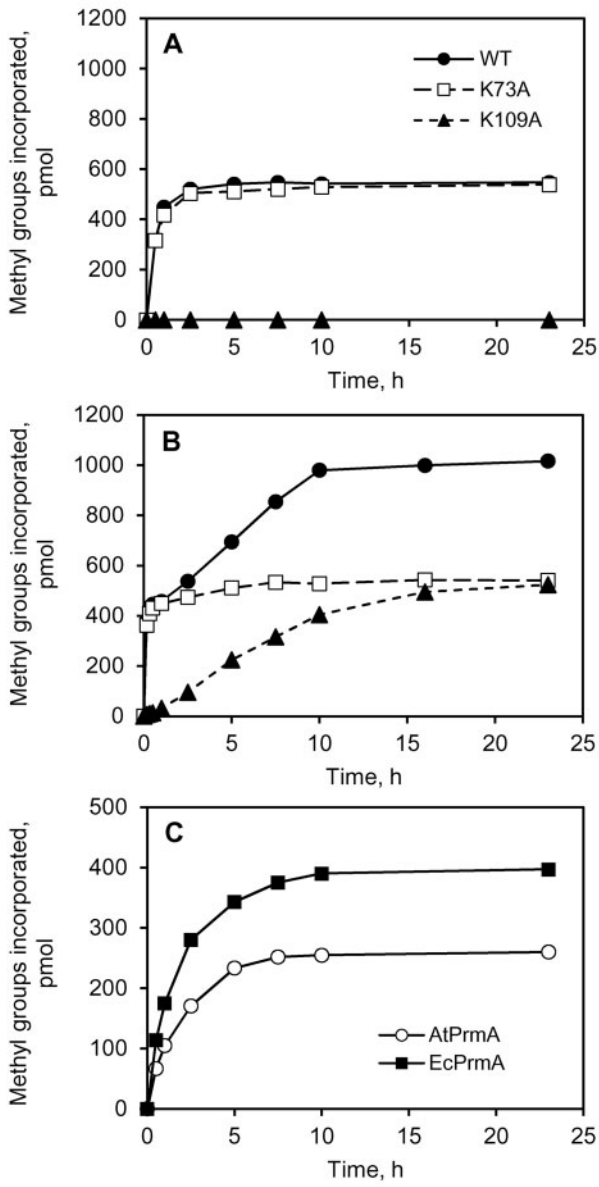

Fig. 7 Methylation of AtPRPL11 and EcRPL11 by AtPrmA and EcPrmA. (A, B) Methylation of wild-type and mutant versions of recombinant AtPRPL11 by AtPrmA (A) or EcPrmA (B). Assays were conducted at 30°C in the presence of AtPRPL11 substrates (3 μg, 170 pmol) and AtPrmA (18 μg) or EcPrmA (12 μg). (C) Methylation of recombinant EcRPL11 by AtPrmA and EcPrmA. Assays were performed at 30°C in the presence of EcPRPL11 (0.7 μg, 45 pmol) and AtPrmA (9 μg) or EcPrmA (6 μg). For all assays, the concentration of [methyl-^{3}H]AdoMet was maintained at about 20 μM and *S*-adenosylhomocysteine hydrolase (100 nM) was included to avoid limitation of the reaction by *S*-adenosylhomocysteine. Kinetics are representative of three determinations.

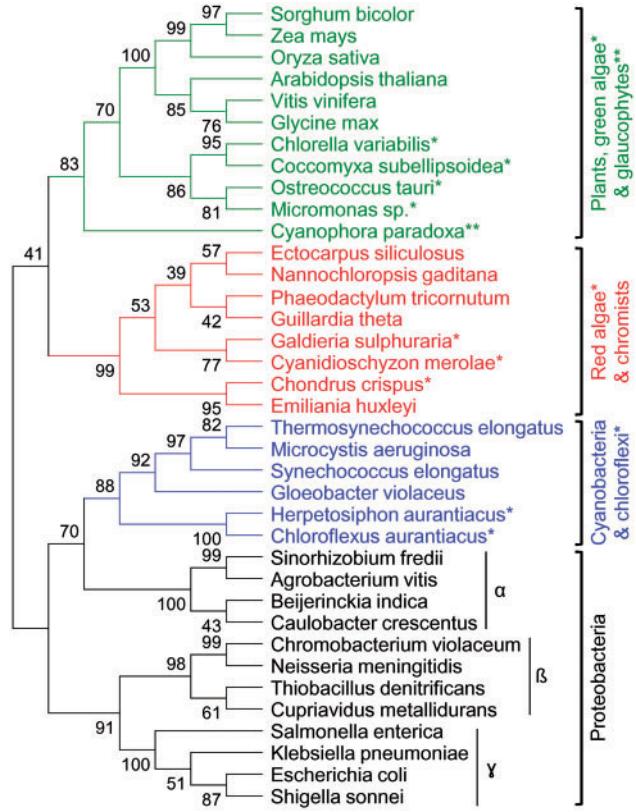

Fig. 8 Phylogenetic analysis of PrmA proteins. The analysis was performed on 37 PrmA protein sequences identified by BlastP search using EcPrmA as a query. Selected sequences covered three bacterial phyla (cyanobacteria, chloroflexi and proteobacteria from alpha, beta, and gamma classes), land plants, chlorophytes (green algae), glaucophytes, rhodophytes (red algae) and chromists (heterokonts, cryptophytes and haptophytes). Accession numbers of the analyzed sequences are available in **Supplementary Table S2**. Sequences were aligned using ClustalW and the phylogenic tree was inferred by using the Maximum Likelihood method based on the Le–Gascuel model (Le and Gascuel 2008). A discrete Gamma distribution was used to model evolutionary rate differences among sites [five categories (+G, parameter = 2.8518)]. The rate variation model allowed for some sites to be evolutionarily invariable ([+I], 3.2634% sites). The consensus bootstrap tree is shown and branch support values (in % for 1,000 replicates) are indicated. Analyses were done with the Mega 6.06 software (Tamura et al. 2013).

gene encoding a protein isoaspartyl *O*-methyltransferase was responsible for the deployment of the protein throughout the cell (cytoplasm, endomembrane system, chloroplasts and/or mitochondria) (Dinkins et al. 2008). Our study provides the first identification and functional characterization of a protein N-methyltransferase with dual localization to plastids and mitochondria. Several protein lysine and arginine methyltransferases have been previously found in chloroplasts, and the substrates for some of them have been identified (Mininno et al. 2012, Alban et al. 2014). To date, the only known mitochondrial methylated protein in plants was Cyt *c* (DiMaria et al. 1982). However, methylation of this substrate is not performed by a mitochondrial enzyme but takes place in the cytoplasm where the apocytochrome *c* is methylated before its import and processing into the organelle (Polevoda et al. 2000). Thus, AtPrmA is the first authentic mitochondrial protein lysine methyltransferase in plants, and it is conceivable, as recently found in humans (Rhein et al. 2013, Rhein et al. 2014), that other protein lysine- or arginine-methylating enzymes are also present in plant mitochondria.

We found that PrmA orthologs are restricted to bacteria and photosynthetic eukaryotes. Our phylogenetic analysis did not discriminate, however, whether eukaryotic *PRMA* genes originate from endosymbiotic or lateral gene transfer. Both evolutionary scenarios seem plausible since lateral gene transfer was shown to play a significant role in the evolution of plastids and that, besides cyanobacteria, the bacterial phyla of chlamydiae and proteobacteria are the most significant sources of genes encoding plastid proteins in eukaryotes (Qiu et al. 2013). Dual targeting of PrmA is likely to be widespread in land plants since a single gene encodes this methyltransferase and the N-termini of precursor PrmA proteins display features of ambiguous transit peptides (Mitschke et al. 2009, Carrie and Small 2013). The situation is less obvious in algae. PrmA proteins from green, red and chromist algae have been analyzed with the PredAlgo program, which is dedicated to multisubcellular localization prediction in green algae (Tardif et al. 2012). Only five out of 14 sequences predicted targeting to chloroplasts (three proteins from green algae) or mitochondria (two proteins from chromists), the others being allocated to other (undefined) compartments using PredAlgo default cutoff values. It is possible, therefore, that dual targeting of PrmA also exists in algae and thus was established early in the evolution of photosynthetic eukaryotes. Experimental evidence will be needed to validate these predictions.

We analyzed the kinetic properties of the Arabidopsis and *E. coli* PrmA enzymes and determined that, despite their evolutionary relationship, these methyltransferases display some differences. Both enzymes have similar product specificity in vitro and in vivo since they make only trimethylated residues (**Table 1**; **Fig. 7**), thus indicating that their active sites are well conserved. This is supported by the high sequence homology (43% identity plus 20% similarity) between the C-terminal catalytic domains of the Arabidopsis and *E. coli* proteins. The plant and bacterial methyltransferases show, however, a difference in substrate site specificity. In vitro, both enzymes share the capacity to catalyze the N-ε-trimethylation of a distal lysine residue embedded in the M(A/E)FCK(D/A)(F/Y)NA motif (**Fig. 7**; **Supplementary Fig. S4**). Unlike EcPrmA, AtPrmA is unable to modify the second internal lysine residue that is proximal to the N-termini of RPL11 substrates (Lys3 in EcRPL11, Lys73 in AtPRPL11). MS/MS data obtained from native plastidial and mitochondrial RPL11 in Col-0 and *prma* lines confirmed these results. Thus, trimethylation of the distal lysine residue occurs in vivo for both Arabidopsis chloroplastic and mitochondrial RPL11 (**Table 1**), but no methylation could be observed in the N-termini of these proteins. For PRPL11, a proximal lysine residue is conserved but not modified in this region, reflecting the enzyme site specificity observed in vitro. For MRPL11, both the AtPrmA properties and the divergence in substrate sequence, in particular the absence of a conserved proximal lysine (**Supplementary Fig. S4**), result in the absence of modification at this site in vivo. Lastly, methylation of the N-terminal residue of RPL11 proteins differs in bacteria and plants. Kinetic analysis with EcRPL11 as a substrate suggests that AtPrmA can trimethylate this site in vitro (**Fig. 7C**), but this result was not confirmed in planta. For MRPL11, Ala2 was found to be N-α-acetylated and for PRPL11 information about the N-terminus of the mature protein is missing. The difference between the plant and bacterial PrmA enzymes could be due to the divergence of their N-terminal substrate recognition module and flexible linker connecting the N- and C-terminal domains. Indeed, these regions display limited sequence conservation (19% identity plus 26% similarity) between AtPrmA and EcPrmA. Thus, it is possible that the binding modes of bacterial and plant enzymes are slightly different and that the mobility of the catalytic domain, which is controlled by the flexible linker, prevents the plant enzyme from modifying the proximal lysine residue of RPL11 substrates. Unfortunately, modeling the tridimensional structure of Arabidopsis PrmA is not sufficient to test this hypothesis since the relative positions of the N- and C-terminal domains differ dramatically in the free and RPL11-complexed structures of the bacterial enzyme (Demirci et al. 2007, Demirci et al. 2008).

RPL11 is an important component of prokaryotic-type ribosomes. It is part of the L7/L12 stalk region of the large subunit, right at the center of this protrusion responsible for the recruitment of initiation, elongation and release factors (Schuwirth et al. 2005, Brown et al. 2014). Thus, the RPL11 arm contributes to the activity of translation factors, and deletion of the protein has important consequences on ribosomal activity in bacteria and organelles (decreased rate of protein synthesis, increased generation time in bacteria or decreased growth rate in plants) (Stark and Cundliffe 1979, Pesaresi et al. 2001, Pesaresi et al. 2006). Despite characterization of *prma*-null mutants in bacteria (Vanet et al. 1994, Cameron et al. 2004) and a higher plant (this work), the biological significance of RPL11 methylation is still not known. Thus, PrmA is dispensable for growth of Arabidopsis in standard environmental conditions (germination, vegetative and reproductive development), and no molecular defect could be associated with the loss of RPL11 methylation in leaf chloroplasts or mitochondria (photosynthetic parameters, steady-state level of organellar-encoded proteins) (**Figs. 2–4**). Also, the overexpression of PrmA in transgenic *prma* 35S::*PRMA* lines (**Fig. 1**) does not modify any of these parameters as compared with wild-type plants. These data, together with the absence of PrmA orthologs in non-photosynthetic eukaryotes and consequently the probable lack of MRPL11 methylation in these organisms, raise the question of the importance of RPL11 methylation for ribosomal function. The analysis of crystal structures from bacterial (Schuwirth et al. 2005) and plastidial (Sharma et al. 2007) ribosomes has allowed us to map methylated sites of RPL11 and to suggest possible roles for these modifications. Thus, the highly conserved trimethylated distal lysine residue is expected to be exposed at the surface of the ribosome (**Supplementary Fig. S5**) and could therefore modulate protein–protein interactions and influence binding of translation factors to the L7/L12 stalk region. The N-terminal residue of RPL11 is less accessible to the solvent or buried within the large subunit, in contact with the rRNA (**Supplementary Fig. S5**). Modification of this residue by either acetylation for MRPL11 or methylation for bacterial, and possibly plastidial, RPL11 may

therefore be involved in protein–RNA interactions and ribosome biogenesis.

It is noteworthy that RPL11 and proteins of the L7/L12 stalk region, namely RPL10 and RPL12, from bacterial and eukaryotic ribosomes have been reported to be phosphorylated on serine or threonine residues, acetylated or methylated at internal lysine residues, and acetylated or methylated at the N-terminus (Koc and Koc 2012, this work). As reported for histones and non-histone proteins, it is possible that these modifications act co-operatively in optimizing ribosome biogenesis and function. Thus, the role played by RPL11 methylation may be revealed if *prma* is combined with other mutations in the genes encoding kinases or acetyltransferases acting on this protein, or on other components of the L7/L12 stalk. To date, the enzymes involved in MRPL11 N-α-acetylation (this work) or PRPL11 phosphorylation on Ser99 (Durek et al. 2010) have not been identified in Arabidopsis. Further studies will be needed to characterize plant RPL11-modifying enzymes and determine a role for methylation, acetylation and phosphorylation of this protein.

Materials and Methods

Plant growth conditions

Wild-type and transgenic *Arabidopsis thaliana* plants of the ecotype Columbia (Col-0) were grown on soil in a growth chamber (22°C, 60% air humidity, light intensity of 80 µmol of photons m^{-2} s^{-1}) under short-day (8 h light) or long-day (16 h light) conditions. Seeds of the T-DNA insertion line SALK_070621 were obtained from the Nottingham Arabidopsis Stock Centre. Seeds for the *prpl11* (Pesaresi et al. 2001) and *mrpl11* (Pesaresi et al. 2006) mutants were kindly provided by Professor Dario Leister (Munchen University, Germany).

Characterization and genetic complementation of the Arabidopsis *prma* mutant

At5g53920 (*prma*) knockout siblings were identified by PCR using genomic DNA isolated from a single leaf and gene-specific and T-DNA-specific primers. Amplicons were sequenced to map the insertion. For RT–PCR experiments, total RNA was isolated from 3-week-old Arabidopsis leaves using the RNeasy plant mini extraction kit (Qiagen). RNA was treated with DNase I and reverse-transcribed with the ThermoScript RT-PCR system (Invitrogen) using oligo(dT). Fragments of the *PRMA* and *ACTIN7* (At5g09810) transcripts were amplified by PCR and analyzed by agarose gel electrophoresis. For genetic complementation, the full-length coding sequence of *PRMA* was fused to a double enhanced 35S promoter using the pFP101 plasmid harboring a green fluorescent protein (GFP) marker (Bensmihen et al. 2004). Homozygous *prma* plants were transformed with this construct by the *Agrobacterium*-mediated floral-dip method (Clough and Bent 1998), and transformed seeds expressing GFP were selected by fluorescence. All primer sequences are available in **Supplementary Table S1**.

Western immunoblotting

Total soluble proteins from Arabidopsis leaves were extracted by grinding samples in 50 mM Tris–HCl, pH 8.0, 1 mM dithiothreitol, 5% (v/v) glycerol and a cocktail of protease inhibitors (Roche Applied Science). Samples were centrifuged at 16,000 × *g* for 20 min at 4°C and the supernatant was used as a source of soluble proteins. Pellets were suspended in the extraction buffer supplemented with 1% (w/v) SDS, incubated for 15 min at room temperature and centrifuged as before to recover solubilized membrane proteins. Proteins were resolved by SDS–PAGE, electroblotted to nitrocellulose membrane and probed using the appropriate antisera. Protein detection was achieved using the ECL Plus™ Western Blotting detection reagents and a Typhoon 9400 scanner (Amersham Biosciences). Polyclonal antibodies against recombinant AtPrmA (Alban et al. 2014) have been produced in guinea pig (Covalab). Antibodies against chloroplastic fructose 1,6 bisphosphate aldolase were from Mininno et al. (2012), and those against light-harvesting antenna complex II, Rubisco large subunit, Cyt *f* and cytochrome oxidase subunit II were obtained from Agrisera (Sweden).

Purification of chloroplasts and mitochondria

Chloroplasts and mitochondria from 5-week-old Arabidopsis rosettes were purified using Percoll density gradients as previously described by Salvi et al. (2008) and Kruft et al. (2001), respectively. Intact organelles were suspended into hypotonic medium (20 mM Tricine, pH 7.6, 1 mM dithiothreitol and protease inhibitors) and submitted to three freeze/thaw cycles to ensure complete lysis. Membranes were separated from soluble proteins (stroma and matrix) by centrifugation at 150,000 × *g* for 30 min at 4°C. Assessment of organelle purity was done by Western blot analyses and by measuring the plastidial NADP-dependent glyceraldehyde 3-phosphate dehydrogenase activity (Sparla et al. 2002). Immunodetection of biotinylated proteins was performed using streptavidin–peroxidase (Puyaubert et al. 2008); the mitochondrial enzyme HPPK-DHPS (Mouillon et al. 2002) and the chloroplastic methyltransferase AtLSMT-L (Mininno et al. 2012) were analyzed using specific antisera. Quantification of Western blots was performed using the ImageQuant TL software (GE Healthcare). Cross-contamination between organellar fractions was ≤5% (see **Supplementary Fig. S2**). A cytosolic-enriched fraction was prepared from Arabidopsis protoplasts as described by Puyaubert et al. (2008).

Germination assays

Germination assays were carried out at 23°C under continuous light (80 µmol of photons m^{-2} s^{-1}) as described in Rajjou et al. (2004). Seeds were incubated in Petri dishes on three sheets of absorbent paper (Whatman) and a membrane filter (ME 24/21 ST, Whatman) imbibed with 1.3 ml of water. The effect of translation inhibitors on germination was analyzed using Col-0 seeds and either cycloheximide (0.1 mM), chloramphenicol (0.6 mM) or spectinomycin (1 mM). Each germination time-course was performed in duplicate (70 seeds per analysis), and four independent seed lots harvested over a 2 year period were analyzed. A seed was considered as germinated when the radicle protruded through the seed coat. Germination parameters (time to reach 50% germination, maximal germination rate) were calculated from fitted curves by using the equation described in Joosen et al. (2010) and Kaleidagraph (Synergy Software).

Photosynthetic parameters

Chl was extracted from leaf tissues in aqueous 80% (v/v) acetone and determined as described in Porra (2002). Chl fluorescence measurements in vivo were performed using a Speedzen MX fluorescence imaging set-up (JBeamBio, Bio-Logic Science Instruments) as described in Allorent et al. (2013, 2015). The parameters F_v/F_m, ΦPSII and non-photochemical quenching were used as indicators of PSII activity in a dark-adapted state, quantum efficiency of the PSII in the light and protection of the photosynthetic machinery from photodamage, respectively. The maximum electron transport rate was deduced from fluorescence recordings as ΦPSII × 0.5 × 0.84 × *I*, where *I* is the incident light in µmol of photons m^{-2} s^{-1}. Statistical analyses were performed with the Kruskal–Wallis and Mann–Whitney tests using the R computing environment (R Development Core Team 2011).

cDNA cloning and site-directed mutagenesis of PRPL11

The coding sequences of *E. coli* PrmA and RPL11 were amplified from genomic DNA (DH5α strain) using the Phusion® high fidelity DNA polymerase (Finnzymes). Primers contained the appropriate restriction sites for cloning into the pET20b(+)expression vector (Novagen) and for the production of N-terminal hexa-His-tagged proteins. The K73A and K109A variants of Arabidopsis PRPL11 were constructed using the Quikchange II site-directed mutagenesis kit (Stratagene) and the pET-PRPL11 plasmid as a template (Alban et al. 2014). Primer sequences are available in **Supplementary Table S1**.

Production and purification of recombinant proteins

Recombinant PrmA proteins were produced in *E. coli* Rosetta-2 cells (Stratagene), whereas RPL11 constructs were introduced into the *E. coli prma*-null mutant KNOK16 (DE3) pRARE2 to avoid any possible methylation by the bacterial PrmA enzyme in vivo (Vanet et al. 1994, Alban et al. 2014). Cells were grown in Luria–Bertani medium at 37°C until mid-log phase, and protein production was induced by the addition of 0.4 mM isopropyl-β-D-thiogalactopyranoside. Incubation was continued for 16 h at 17°C and cells were collected by centrifugation (4,000 × *g*, 20 min). For all recombinant proteins except EcRPL11, cells were suspended in buffer A (50 mM Tris–HCl, pH 8.0, 0.5 M NaCl, 10 mM imidazole and a cocktail of protease inhibitors), sonicated, and His-tagged proteins were purified from the soluble protein extracts by chromatography onto an Ni Sepharose 6 Fast Flow (GE Healthcare Bio-Sciences) column according to the procedure described previously (Alban et al. 2014). EcRPL11 was mainly insoluble and purified from inclusion bodies. Extensively washed inclusion bodies were solubilized in buffer B (25 mM Tris–HCl, pH 8.0, 10 mM $MgCl_2$, 0.4 M NaCl) supplemented with 6 M urea and purified on an Ni Sepharose column under denaturing conditions. Refolding was done by dialysis against buffer B containing 0.5 mM EDTA, as previously described (Holmberg and Noller 1999, Jenvert and Schiavone 2007).

Methylation assays

The incorporation of methyl groups from AdoMet into RPL11 substrates was determined as described previously (Colson 1977, Mininno et al. 2012, Alban et al. 2014). Assay mixtures contained 0.6 M potassium acetate (pH 7.8), 20 μM [methyl-^{3}H]AdoMet (70–85 Ci mmol^{-1}; PerkinElmer Life Sciences), 100 nM *S*-adenosylhomocysteine hydrolase (Sigma-Aldrich), PrmA (recombinant or native enzymes from chloroplasts or mitochondria) and protein substrates (recombinant proteins or Arabidopsis extracts). Reactions were conducted at 30°C and terminated by the addition of 500 μl of trichloroacetic acid 10% (w/v) and 5 μl of sodium deoxycholate 1% (w/v). Radioactivity incorporated into proteins was determined by liquid scintillation counting and/or by phosphorimaging. For phosphorimage analyses, proteins were resolved by SDS–PAGE, transferred to ProBlott membranes (Applied Biosystems) and exposed to a tritium storage phosphor screen (Molecular Dynamics) for 5–10 d before detection using a Typhoon 9400 scanner (Amersham Biosciences).

Mass spectrometry methods

In-gel protein digestion with trypsin was carried out using a Freedom EVO150 robotic platform (TECAN Lyon) as described previously (Alban et al. 2014). Nano-LC-MS/MS raw data were acquired on an LTQ-Orbitrap Velos hybrid mass spectrometer (ThermoFisher Scientific) as described in Mininno et al. (2012). Gel bands from the mitochondrial samples were analyzed using an Inclusion List containing all possible *m/z* ratios (±10 p.p.m.) of precursor ions that could encompass the Lys48 residue of MRPL11 (**Supplementary Fig. S3**). Peak lists were generated with Mascot Distiller 2.5.1 (Matrix Science) from the LC-MS/MS raw data. MS/MS spectra were searched using Mascot 2.4.1 (Matrix Science) against the target-decoy version of a compilation of the *A. thaliana* protein database (nuclear, mitochondrial and plastid genome; TAIR v10.0; December 14, 2010; 35,386 entries) and a home-made list of contaminants frequently observed in proteomics analyses (260 entries). Up to two trypsin miscleavages were allowed. Acetyl (protein N-α-acetylation), methionine oxidation and dioxidation, methyl (lysine and arginine), dimethyl (lysine and arginine) and trimethyl (lysine) were searched at the same time as variable modifications. In addition, carbamidomethyl cysteine was set as a fixed modification. Mascot search results were automatically filtered as described in Alban et al. (2014) with the IRMa 1.31.1 software. Only peptides ranked first and with a homology threshold *P*-value < 0.1 were kept. Spectra of interest were checked manually to confirm the sequence and modifications.

Phylogenetic analyses

Proteins orthologous to EcPrmA were identified by BlastP searches at the NCBI using the non-redundant protein sequences database from archaea, bacteria and eukaryotes. All phylogenetic analyses were conducted using the Molecular Evolutionary Genetics Analysis software (Mega 6.06) (Tamura et al. 2013). First, sequences were aligned using ClustalW and the best model of sequence evolution was identified. Then, maximum likelihood- (ML) based phylogenetic analyses were performed using the Le–Gascuel model (Le and Gascuel, 2008) and a discrete Gamma distribution with five rate categories. The rate variation model allowed for some sites to be evolutionarily invariable. Branch consistency supports were evaluated using 1,000 bootstrap replicates.

Supplementary data

Supplementary data are available at PCP online.

Funding

This work was supported by the Department of Plant Biology from the Institut National de la Recherche Agronomique; the Proteomics French Infrastructure [ANR-10-INBS-08-01]; the University Grenoble Alpes [PhD fellowship to M. Mininno.].

Acknowledgements

The authors gratefully acknowledge Dr. Giovanni Finazzi (LPCV, Grenoble) for advice on Chl fluorescence analysis, and Jean-Pierre Andrieu (platform of the Partnership for Structural Biology and the Institut de Biologie Structurale, Grenoble, France) for assistance and access to the protein sequencing facility. We thank Professor. Dario Leister (Munich University) for providing us with *prpl11* and *mrpl11* seeds. We acknowledge Drs. Jacques Bourguignon and Florent Villiers (LPCV, Grenoble) for fruitful discussions and critical reading of the manuscript.

Disclosures

The authors have no conflicts of interest to declare.

References

Alban, C., Tardif, M., Mininno, M., Brugiere, S., Gilgen, A., Ma, S., et al. (2014) Uncovering the protein lysine and arginine methylation network in Arabidopsis chloroplasts. *PLoS One* 9: e95512.

Al-Hadid, Q., Roy, K., Munroe, W., Dzialo, M.C., Chanfreau, G.F. and Clarke, S.G. (2014) Histidine methylation of yeast ribosomal protein Rpl3p is required for proper 60S subunit assembly. *Mol. Cell. Biol.* 34: 2903–2916.

Allorent, G., Osorio, S., Vu, J.L., Falconet, D., Jouhet, J., Kuntz, M., et al. (2015) Adjustments of embryonic photosynthetic activity modulate seed fitness in Arabidopsis thaliana. *New Phytol.* 205: 707–719.

Allorent, G., Tokutsu, R., Roach, T., Peers, G., Cardol, P., Girard-Bascou, J., et al. (2013) A dual strategy to cope with high light in Chlamydomonas reinhardtii. *Plant Cell* 25: 545–557.

Bensmihen, S., To, A., Lambert, G., Kroj, T., Giraudat, J. and Parcy, F. (2004) Analysis of an activated ABI5 allele using a new selection method for transgenic Arabidopsis seeds. *FEBS Lett.* 561: 127–131.

Bonen, L. and Calixte, S. (2006) Comparative analysis of bacterial-origin genes for plant mitochondrial ribosomal proteins. *Mol. Biol. Evol.* 23: 701–712.

Brown, A., Amunts, A., Bai, X.C., Sugimoto, Y., Edwards, P.C., Murshudov, G., et al. (2014) Structure of the large ribosomal subunit from human mitochondria. *Science* 346: 718–722.

Cameron, D.M., Gregory, S.T., Thompson, J., Suh, M.J., Limbach, P.A. and Dahlberg, A.E. (2004) Thermus thermophilus L11 methyltransferase, PrmA, is dispensable for growth and preferentially modifies free ribosomal protein L11 prior to ribosome assembly. *J. Bacteriol.* 186: 5819–5825.

Carrie, C. and Small, I. (2013) A reevaluation of dual-targeting of proteins to mitochondria and chloroplasts. *Biochim. Biophys. Acta* 1833: 253–259.

Carroll, A.J. (2013) The Arabidopsis cytosolic ribosomal proteome: from form to function. *Front. Plant Sci.* 4: 32.

Carroll, A.J., Heazlewood, J.L., Ito, J. and Millar, A.H. (2008) Analysis of the Arabidopsis cytosolic ribosome proteome provides detailed insights into its components and their post-translational modification. *Mol. Cell. Proteomics* 7: 347–369.

Chern, M.K., Chang, K.N., Liu, L.F., Tam, T.C., Liu, Y.C., Liang, Y.L., et al. (2002) Yeast ribosomal protein L12 is a substrate of protein-arginine methyltransferase 2. *J. Biol. Chem.* 277: 15345–15353.

Clarke, S.G. (2013) Protein methylation at the surface and buried deep: thinking outside the histone box. *Trends Biochem. Sci.* 38: 243–252.

Clough, S.J. and Bent, A.F. (1998) Floral dip: a simplified method for Agrobacterium-mediated transformation of Arabidopsis thaliana. *Plant J.* 16: 735–743.

Colson, C. (1977) Genetics of ribosomal protein methylation in *Escherichia coli*. I. A mutant deficient in methylation of protein L11. *Mol. Gen. Genet.* 154: 167–173.

Demirci, H., Gregory, S.T., Dahlberg, A.E. and Jogl, G. (2007) Recognition of ribosomal protein L11 by the protein trimethyltransferase PrmA. *EMBO J.* 26: 567–577.

Demirci, H., Gregory, S.T., Dahlberg, A.E. and Jogl, G. (2008) Multiple-site trimethylation of ribosomal protein L11 by the PrmA methyltransferase. *Structure* 16: 1059–1066.

DiMaria, P., Kim, S. and Paik, W.K. (1982) Cytochrome c specific methylase from wheat germ. *Biochemistry* 21: 1036–1044.

Dinkins, R.D., Majee, S.M., Nayak, N.R., Martin, D., Xu, Q., Belcastro, M.P., et al. (2008) Changing transcriptional initiation sites and alternative 5′- and 3′-splice site selection of the first intron deploys Arabidopsis protein isoaspartyl methyltransferase2 variants to different subcellular compartments. *Plant J.* 55: 1–13.

Dognin, M.J. and Wittmann-Liebold, B. (1980) Purification and primary structure determination of the N-terminal blocked protein, L11, from *Escherichia coli* ribosomes. *Eur. J. Biochem.* 112: 131–151.

Dorrell, R.G. and Smith, A.G. (2011) Do red and green make brown? Perspectives on plastid acquisitions within chromalveolates. *Eukaryot. Cell* 10: 856–868.

Durek, P., Schmidt, R., Heazlewood, J.L., Jones, A., MacLean, D., Nagel, A., et al. (2010) PhosPhAt: the Arabidopsis thaliana phosphorylation site database. An update. *Nucleic Acids Res* 38: D828–D834.

Emanuelsson, O., Nielsen, H., Brunak, S. and von Heijne, G. (2000) Predicting subcellular localization of proteins based on their N-terminal amino acid sequence. *J. Mol. Biol.* 300: 1005–1016.

Galland, M., Boutet-Mercey, S., Lounifi, I., Godin, B., Balzergue, S., Grandjean, O., et al. (2014) Compartmentation and dynamics of flavone metabolism in dry and germinated rice seeds. *Plant Cell Physiol.* 55: 1646–1659.

Holmberg, L. and Noller, H.F. (1999) Mapping the ribosomal RNA neighborhood of protein L11 by directed hydroxyl radical probing. *J. Mol. Biol.* 289: 223–233.

Jenvert, R.M. and Schiavone, L.H. (2007) The flexible N-terminal domain of ribosomal protein L11 from *Escherichia coli* is necessary for the activation of stringent factor. *J. Mol. Biol.* 365: 764–772.

Joosen, R.V., Kodde, J., Willems, L.A., Ligterink, W., van der Plas, L.H. and Hilhorst, H.W. (2010) GERMINATOR: a software package for high-throughput scoring and curve fitting of Arabidopsis seed germination. *Plant J.* 62: 148–159.

Kaundal, R., Saini, R. and Zhao, P.X. (2010) Combining machine learning and homology-based approaches to accurately predict subcellular localization in Arabidopsis. *Plant Physiol.* 154: 36–54.

Koc, E.C. and Koc, H. (2012) Regulation of mammalian mitochondrial translation by post-translational modifications. *Biochim. Biophys. Acta* 1819: 1055–1066.

Kruft, V., Eubel, H., Jansch, L., Werhahn, W. and Braun, H.P. (2001) Proteomic approach to identify novel mitochondrial proteins in Arabidopsis. *Plant Physiol.* 127: 1694–1710.

Le, S.Q. and Gascuel, O. (2008) An improved general amino acid replacement matrix. *Mol. Biol. Evol.* 25: 1307–1320.

Mininno, M., Brugiere, S., Pautre, V., Gilgen, A., Ma, S., Ferro, M., et al. (2012) Characterization of chloroplastic fructose 1,6-bisphosphate aldolases as lysine-methylated proteins in plants. *J. Biol. Chem.* 287: 21034–21044.

Mitschke, J., Fuss, J., Blum, T., Hoglund, A., Reski, R., Kohlbacher, O., et al. (2009) Prediction of dual protein targeting to plant organelles. *New Phytol.* 183: 224–235.

Mouillon, J.M., Ravanel, S., Douce, R. and Rebeille, F. (2002) Folate synthesis in higher-plant mitochondria: coupling between the dihydropterin pyrophosphokinase and the dihydropteroate synthase activities. *Biochem. J.* 363: 313–319.

Nesterchuk, M.V., Sergiev, P.V. and Dontsova, O.A. (2011) Posttranslational modifications of ribosomal proteins in *Escherichia coli*. *Acta Naturae* 3: 22–33.

Pesaresi, P., Masiero, S., Eubel, H., Braun, H.P., Bhushan, S., Glaser, E., et al. (2006) Nuclear photosynthetic gene expression is synergistically modulated by rates of protein synthesis in chloroplasts and mitochondria. *Plant Cell* 18: 970–991.

Pesaresi, P., Varotto, C., Meurer, J., Jahns, P., Salamini, F. and Leister, D. (2001) Knock-out of the plastid ribosomal protein L11 in Arabidopsis: effects on mRNA translation and photosynthesis. *Plant J.* 27: 179–189.

Polevoda, B., Martzen, M.R., Das, B., Phizicky, E.M. and Sherman, F. (2000) Cytochrome c methyltransferase, Ctm1p, of yeast. *J. Biol. Chem.* 275: 20508–20513.

Polevoda, B. and Sherman, F. (2007) Methylation of proteins involved in translation. *Mol. Microbiol.* 65: 590–606.

Porra, R.J. (2002) The chequered history of the development and use of simultaneous equations for the accurate determination of chlorophylls a and b. *Photosynth. Res.* 73: 149–156.

Porras-Yakushi, T.R., Whitelegge, J.P., Miranda, T.B. and Clarke, S. (2005) A novel SET domain methyltransferase modifies ribosomal protein Rpl23ab in yeast. *J. Biol. Chem.* 280: 34590–34598.

Puyaubert, J., Denis, L. and Alban, C. (2008) Dual targeting of Arabidopsis holocarboxylase synthetase1: a small upstream open reading frame regulates translation initiation and protein targeting. *Plant Physiol.* 146: 478–491.

Qiu, H., Price, D.C., Weber, A.P., Facchinelli, F., Yoon, H.S. and Bhattacharya, D. (2013) Assessing the bacterial contribution to the plastid proteome. *Trends Plant Sci.* 18: 680–687.

R Development Core Team (2011) R: A Language and Environment for Statistical Computing. R Foundation for Statistical Computing, Vienna, Austria.

Rajjou, L., Duval, M., Gallardo, K., Catusse, J., Bally, J., Job, C., et al. (2012) Seed germination and vigor. *Annu. Rev. Plant Biol.* 63: 507–533.

Rajjou, L., Gallardo, K., Debeaujon, I., Vandekerckhove, J., Job, C. and Job, D. (2004) The effect of alpha-amanitin on the Arabidopsis seed proteome highlights the distinct roles of stored and neosynthesized mRNAs during germination. *Plant Physiol.* 134: 1598–1613.

Rhein, V.F., Carroll, J., Ding, S., Fearnley, I.M. and Walker, J.E. (2013) NDUFAF7 methylates arginine 85 in the NDUFS2 subunit of human complex I. *J. Biol. Chem.* 288: 33016–33026.

Rhein, V.F., Carroll, J., He, J., Ding, S., Fearnley, I.M. and Walker, J.E. (2014) Human METTL20 methylates lysine residues adjacent to the

recognition loop of the electron transfer flavoprotein in mitochondria. *J. Biol. Chem.* 289: 24640–24651.

Salvi, D., Rolland, N., Joyard, J. and Ferro, M. (2008) Purification and proteomic analysis of chloroplasts and their sub-organellar compartments. *Methods Mol. Biol.* 432: 19–36.

Schuwirth, B.S., Borovinskaya, M.A., Hau, C.W., Zhang, W., Vila-Sanjurjo, A., Holton, J.M., et al. (2005) Structures of the bacterial ribosome at 3.5 Å resolution. *Science* 310: 827–834.

Sharma, M.R., Wilson, D.N., Datta, P.P., Barat, C., Schluenzen, F., Fucini, P., et al. (2007) Cryo-EM study of the spinach chloroplast ribosome reveals the structural and functional roles of plastid-specific ribosomal proteins. *Proc. Natl Acad. Sci. USA* 104: 19315–19320.

Small, I., Peeters, N., Legeai, F. and Lurin, C. (2004) Predotar: a tool for rapidly screening proteomes for N-terminal targeting sequences. *Proteomics* 4: 1581–1590.

Sparla, F., Pupillo, P. and Trost, P. (2002) The C-terminal extension of glyceraldehyde-3-phosphate dehydrogenase subunit B acts as an autoinhibitory domain regulated by thioredoxins and nicotinamide adenine dinucleotide. *J. Biol. Chem.* 277: 44946–44952.

Stark, M. and Cundliffe, E. (1979) On the biological role of ribosomal protein BM-L11 of Bacillus megaterium, homologous with *Escherichia coli* ribosomal protein L11. *J. Mol. Biol.* 134: 767–769.

Stiller, J.W., Schreiber, J., Yue, J., Guo, H., Ding, Q. and Huang, J. (2014) The evolution of photosynthesis in chromist algae through serial endosymbioses. *Nat. Commun.* 5: 5764.

Tamura, K., Stecher, G., Peterson, D., Filipski, A. and Kumar, S. (2013) MEGA6: Molecular Evolutionary Genetics Analysis version 6.0. *Mol. Biol. Evol.* 30: 2725–2729.

Tanz, S.K., Castleden, I., Hooper, C.M., Vacher, M., Small, I. and Millar, H.A. (2013) SUBA3: a database for integrating experimentation and prediction to define the SUBcellular location of proteins in Arabidopsis. *Nucleic Acids Res* 41: D1185–D1191.

Tardif, M., Atteia, A., Specht, M., Cogne, G., Rolland, N., Brugiere, S., et al. (2012) PredAlgo: a new subcellular localization prediction tool dedicated to green algae. *Mol. Biol. Evol.* 29: 3625–3639.

Vanet, A., Plumbridge, J.A., Guerin, M.F. and Alix, J.H. (1994) Ribosomal protein methylation in *Escherichia coli*: the gene prmA, encoding the ribosomal protein L11 methyltransferase, is dispensable. *Mol. Microbiol.* 14: 947–958.

Webb, K.J., Lipson, R.S., Al-Hadid, Q., Whitelegge, J.P. and Clarke, S.G. (2010a) Identification of protein N-terminal methyltransferases in yeast and humans. *Biochemistry* 49: 5225–5235.

Webb, K.J., Zurita-Lopez, C.I., Al-Hadid, Q., Laganowsky, A., Young, B.D., Lipson, R.S., et al. (2010b) A novel 3-methylhistidine modification of yeast ribosomal protein Rpl3 is dependent upon the YIL110W methyltransferase. *J. Biol. Chem.* 285: 37598–37606.

Yamaguchi, K. and Subramanian, A.R. (2000) The plastid ribosomal proteins. Identification of all the proteins in the 50S subunit of an organelle ribosome (chloroplast). *J. Biol. Chem.* 275: 28466–28482.

Yamaguchi, K., von Knoblauch, K. and Subramanian, A.R. (2000) The plastid ribosomal proteins. Identification of all the proteins in the 30S subunit of an organelle ribosome (chloroplast). *J. Biol. Chem.* 275: 28455–28465.

Young, B.D., Weiss, D.I., Zurita-Lopez, C.I., Webb, K.J., Clarke, S.G. and McBride, A.E. (2012) Identification of methylated proteins in the yeast small ribosomal subunit: a role for SPOUT methyltransferases in protein arginine methylation. *Biochemistry* 51: 5091–5104.